

NEO: A Novel Expeditious Optimisation Algorithm for Reactive Motion Control of Manipulators

Jesse Haviland¹, Peter Corke¹

Abstract—We present NEO, a fast and purely reactive motion controller for manipulators which can avoid static and dynamic obstacles while moving to the desired end-effector pose. Additionally, our controller maximises the manipulability of the robot during the trajectory, while avoiding joint position and velocity limits. NEO is wrapped into a strictly convex quadratic programme which, when considering obstacles, joint limits, and manipulability on a 7 degree-of-freedom robot, is generally solved in a few ms. While NEO is not intended to replace state-of-the-art motion planners, our experiments show that it is a viable alternative for scenes with moderate complexity while also being capable of reactive control. For more complex scenes, NEO is better suited as a reactive local controller, in conjunction with a global motion planner. We compare NEO to motion planners on a standard benchmark in simulation and additionally illustrate and verify its operation on a physical robot in a dynamic environment. We provide an open-source library which implements our controller.

I. INTRODUCTION

The real world is not static and consequently, manipulators must be up to the challenge of reacting to the unpredictable nature of the environment they work in. Getting a manipulator's end-effector from point A to point B is a fundamental problem in robotic control. While the task is seemingly simple, there can be numerous causes of failure, especially as the environment becomes cluttered and dynamic. Dynamic obstacle avoidance is essential for manipulators to be robust in such environments.

Each iteration of the control loop must be able to consider the state of both environment and robot to guarantee safe and reliable robot operation. The current focus in obstacle avoidance for manipulators has come at the cost of greater up-front computational load, leading to open-loop or semi-closed loop controllers. Reliably avoiding non-stationary obstacles requires a reactive approach. Planners compute a sequence of joint coordinates which at run time become joint velocities, while a reactive approach works purely with joint velocities.

We start by considering the differential kinematics. A set of joint velocities can be computed such that the end-effector will achieve a desired Cartesian velocity towards the goal. This classic and purely reactive approach is known as resolved-rate motion control (RRMC). Using this technique, the end-effector is effectively *steered* in a straight-line, in

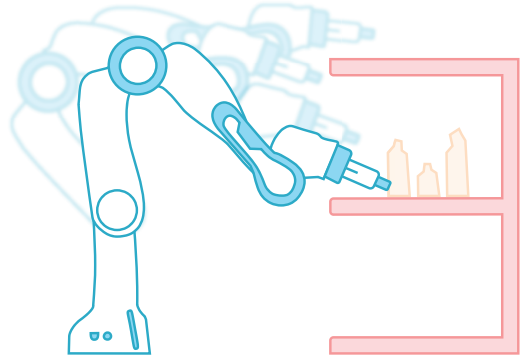


Fig. 1: Our NEO controller drives a robot's joint velocities such that the robot does not collide with obstacles (that may be non-stationary), does not exceed joint position or velocity limits and maximises the manipulability of the robot, purely reactively.

Cartesian space, towards the goal pose. The first benefit of this approach is that it is cheap to compute and easily able to run at over 1000 Hz. By reformulating the traditional RRMC algorithm, we can add additional capabilities while maintaining its purely reactive nature.

Differential kinematics also allows us to capture the rate of change of the distance between any part of the robot and any obstacle present in the environment. By exploiting such a relationship, a reactive controller can be developed that will avoid colliding with obstacles. However, the resulting controller may be over-constrained and unable to achieve the goal pose, and we can employ two strategies to resolve this.

Firstly, kinematically redundant manipulators have more degrees of freedom than is necessary to reach any pose within their task space. Until recently redundant manipulators for industrial or research use were rare but are now increasingly common. Secondly, we can relax the path specification to allow for intentional error, called slack. Slack allows the end-effector to diverge from the straight-line trajectory to dodge obstacles.

To provide the best chance for the robot to be able to react in a volatile environment, we must consider the robot's conditioning. A measure of manipulability, devised in [1], describes how well-conditioned a manipulator is to achieve any arbitrary velocity. Therefore, by also maximising the manipulability of the robot, we can decrease the likelihood of robot failure due to singularity while also improving robot obstacle avoidance.

The contributions of this paper are:

¹Jesse Haviland and Peter Corke are with the Australian Centre for Robotic Vision (ACRV), Queensland University of Technology Centre for Robotics (QCR), Brisbane, Australia j.haviland@qut.edu.au, peter.corke@qut.edu.au. This research was conducted by the Australian Research Council project number CE140100016, and supported by the QUT Centre for Robotics.

- 1) a reactive motion controller for serial-link manipulators (fully actuated or redundant) that can achieve a desired end-effector pose with the ability to dodge stationary and non-stationary obstacles, avoid joint limits and maximise manipulability.
- 2) experimental validation in simulation on a published motion planning benchmark as well as on a physical Franka-Emika Panda robot. [jhavl.github.io/neo](https://github.com/jhavl/neo).

II. RELATED WORK

Planning a collision free-path in a cluttered scene can be computationally expensive. Classical planning approaches include rapidly-exploring random trees [2] and probabilistic roadmaps [3]. These methods will find the optimal path according to the supplied criteria. However, their computation time means they are restricted to use as offline planners.

Motion planners such as STOMP [4], CHOMP [5] and Trajopt [6] use such sampling-based methods to solve general high-dimensional motion planning problems not just for manipulators. Motion planners can typically incorporate collision avoidance as well as other constraints such as end-effector orientation throughout the motion. In some cases, motion-planners may need post-processing to remove jerky or extraneous motions due to sampling.

STOMP uses a stochastic and gradient-free scheme to optimize a trajectory while minimizing a cost function. The stochastic nature of the scheme means that it can overcome local minima which purely gradient-based approaches like CHOMP and Trajopt can be trapped by. CHOMP and Trajopt both utilise novel methods for solving optimisation problems while incorporating obstacles.

The time to run these systems makes it impossible for them to run reliably in dynamic environments due to the need for frequent replanning. Planning times of these planners in one benchmark [6] vary from 0.19 seconds (for Trajopt) to 4.91 seconds (for CHOMP). If the obstacles in the environment are non-stationary, the planners will not be able to re-plan at a sufficient rate to avoid them.

Path planners output a sequence of poses for which the inverse kinematic (IK) solution is computed to obtain a sequence of joint coordinates. IK can be solved analytically on most robots, but it is more commonly solved through an optimization framework [7]. The optimization problem can be augmented through the cost function, equality or inequality constraints to provide additional functionality. IK solvers can therefore provide joint configurations which are free from collisions and avoid joint limits. Typically only redundant robots with an exploitable null space can achieve useful benefits.

However, IK alone cannot provide a valid path to the goal. Rather than consider the pose or joint configuration at each time step we can consider velocity. This approach, using differential kinematics, is commonly referred to as Resolved-Rate Motion Control (RRMC) [8].

RRMC uses the derivative of the forward kinematics to choose joint velocities which will drive the robot in a straight

line from the starting end-effector pose to the desired end-effector pose. Unlike the previously mentioned approaches, RRMC is purely reactive and provides the joint velocities for the next time instant rather than for the whole trajectory.

If the robot is redundant, there are an infinite set of joint velocities which will achieve the desired end-effector velocity. Some additional constraint is required, typically minimising the norm of joint velocity. Alternatively, through gradient projection and exploitation of the null space, the robot can complete sub-tasks while achieving its motion. One such subtask is maximising the manipulability of the robot [9]. By projecting the manipulability Jacobian into the null space of the differential kinematic equation, the manipulator will perform the straight-line end-effector motion towards the goal pose, but also choose joint velocities such that the robot manipulability is maximised at each step. This is beneficial for the robustness of the robot operation as it decreases the likelihood the robot will approach configuration. In a dynamic environment, the required motion can be in any direction, which means that an isotropic velocity capability is advantageous.

RRMC can be reformulated as a quadratic programming (QP) optimisation problem. QPs provide the ability to consider constraints and costs which add additional functionality. The work in [10] incorporated the physical joint limits of a mobile manipulator into a QP. Additionally, recent work in [11] introduced slack into the typical straight-line approach of RRMC. The slack effectively introduces extra redundancy to the problem which is especially useful for robots with six or less degrees-of-freedom. This work then exploited the extra redundancy to maximise the manipulability and avoid physical joint limits of manipulators through a reactive QP controller. The velocity damper approach described in [12] was used to avoid joint limits but could equally be used to avoid obstacles.

An alternate approach to reactive motion control is through potential fields where the robot is repelled from joint limits and obstacles [13]. However, this approach does not lend itself well to improving the manipulability of the robot.

The benefit of reactive controllers is that they can be utilised for control techniques such as visual servoing [14] and closed-loop visual grasping [15]. Visual servoing directly provides the end-effector velocity which must be followed and is updated on each iteration of the vision control loop. This makes it difficult to integrate with planning-based methods.

This paper proposes a novel real-time motion controller which can avoid moving obstacles (for the whole robot, not just the end-effector), avoid physical joint limits and maximises the manipulability of a manipulator in a purely reactive manner.

In Section III we incorporate the differential kinematics and manipulability maximisation into a general quadratic programming problem. We detail how obstacles can be incorporated in Section IV. We then show that velocity dampers and introducing slack can be used to effectively dodge obstacles in Section V. The NEO controller is then

defined in Section VI. Section VII describes our experimental setup and methodology. Finally, Section VIII details our experimental results and insights informed by the results.

III. QUADRATIC PROGRAMMING

The generic form of a QP is [16]

$$\begin{aligned} \min_{\mathbf{x}} \quad & f_o(\mathbf{x}) = \frac{1}{2} \mathbf{x}^\top \mathbf{Q} \mathbf{x} + \mathbf{c}^\top \mathbf{x}, \\ \text{subject to} \quad & \mathbf{A}_1 \mathbf{x} = \mathbf{b}_1, \\ & \mathbf{A}_2 \mathbf{x} \leq \mathbf{b}_2, \\ & \mathbf{d} \leq \mathbf{x} \leq \mathbf{e}. \end{aligned} \quad (1)$$

where f_o is the objective function to minimise; \mathbf{A}_1 , \mathbf{b}_1 define the equality constraints; \mathbf{A}_2 , \mathbf{b}_2 define the inequality constraints, and \mathbf{d} and \mathbf{e} define the lower and upper bounds of the optimisation variable \mathbf{x} . One benefit of QPs is that they are strictly convex when the matrix \mathbf{Q} is positive definite [16].

A. Incorporating the Differential Kinematics into a QP

The first-order differential kinematics for a serial-link manipulator are described by

$$\boldsymbol{\nu}(t) = \mathbf{J}(\mathbf{q}) \dot{\mathbf{q}}(t) \quad (2)$$

where

$$\boldsymbol{\nu}(t) = (v_x \ v_y \ v_z \ \omega_x \ \omega_y \ \omega_z)^\top \in \mathbb{R}^6 \quad (3)$$

is the end-effector spatial velocity and $\mathbf{J}(\mathbf{q}) \in \mathbb{R}^{6 \times n}$ is the manipulator Jacobian which relates the end-effector spatial velocity $\boldsymbol{\nu}$ to the joint velocities $\dot{\mathbf{q}}(t)$, and n is the number of joints in the robot.

We can incorporate (2) into a quadratic program as

$$\begin{aligned} \min_{\dot{\mathbf{q}}} \quad & f_o(\dot{\mathbf{q}}) = \frac{1}{2} \dot{\mathbf{q}}^\top \mathbf{I} \dot{\mathbf{q}}, \\ \text{subject to} \quad & \mathbf{J}(\mathbf{q}) \dot{\mathbf{q}} = \boldsymbol{\nu}, \\ & \dot{\mathbf{q}}^- \leq \dot{\mathbf{q}} \leq \dot{\mathbf{q}}^+ \end{aligned} \quad (4)$$

where \mathbf{I} is an $n \times n$ identity matrix, $\dot{\mathbf{q}}^-$ and $\dot{\mathbf{q}}^+$ represent the upper and lower joint-velocity limits, and no inequality constraints need to be defined. If the robot has more degrees-of-freedom than necessary to reach its entire task space, the QP in (4) will achieve the desired end-effector velocity with the minimum joint velocity norm. However, there are other things we can optimise for, such as manipulability.

B. Incorporating Manipulability into a QP

The manipulability measure, devised in [1], describes the conditioning of a manipulator, or how easily the robot can achieve any arbitrary velocity. The manipulability measure is a scalar

$$m = \sqrt{\det(\mathbf{J}(\mathbf{q}) \mathbf{J}(\mathbf{q})^\top)} \quad (5)$$

We can consider the measure as the distance to a kinematic singularity where the manipulator Jacobian becomes rank deficient – disallowing motion in certain task-space directions. A symptom of approaching a singularity is that the required

joint velocities reach impossible levels [17]. During reactive control in dynamic environments, where the direction of the next step is not known ahead of time, isotropic velocity control is of paramount importance.

We can use the time derivative of (5) and incorporate it into the QP in (4) to maximise manipulability while still achieving the desired end-effector velocity [11]

$$\begin{aligned} \min_{\dot{\mathbf{q}}} \quad & f_o(\dot{\mathbf{q}}) = \underbrace{\frac{1}{2} \dot{\mathbf{q}}^\top (\lambda_q \mathbf{I}) \dot{\mathbf{q}}}_A - \underbrace{\mathbf{J}_m^\top \dot{\mathbf{q}}}_B, \\ \text{subject to} \quad & \underbrace{\mathbf{J}(\mathbf{q}) \dot{\mathbf{q}} = \boldsymbol{\nu}}_C, \\ & \underbrace{\dot{\mathbf{q}}^- \leq \dot{\mathbf{q}} \leq \dot{\mathbf{q}}^+}_D \end{aligned} \quad (6)$$

- A – Minimises the norm of the velocity
- B – Maximises the manipulability of the robot
- C – Ensures the desired end-effector velocity
- D – Ensures the the robot's velocity limits are respected

where λ_q is the gain for velocity-norm minimisation, and $\mathbf{J}_m \in \mathbb{R}^n$ is the manipulability Jacobian which relates the rate of change of manipulability to the joint velocities

$$\mathbf{J}_m^\top = \begin{pmatrix} m \operatorname{vec}(\mathbf{J} \mathbf{H}_1^\top)^\top \operatorname{vec}((\mathbf{J} \mathbf{J}^\top)^{-1}) \\ m \operatorname{vec}(\mathbf{J} \mathbf{H}_2^\top)^\top \operatorname{vec}((\mathbf{J} \mathbf{J}^\top)^{-1}) \\ \vdots \\ m \operatorname{vec}(\mathbf{J} \mathbf{H}_n^\top)^\top \operatorname{vec}((\mathbf{J} \mathbf{J}^\top)^{-1}) \end{pmatrix} \quad (7)$$

with $\mathbf{J}_m^\top \in \mathbb{R}^n$ and where the vector operation $\operatorname{vec}(\cdot) : \mathbb{R}^{a \times b} \rightarrow \mathbb{R}^{ab}$ converts a matrix column-wise into a vector, and $\mathbf{H}_i \in \mathbb{R}^{6 \times n}$ is the i^{th} component of the manipulator Hessian tensor $\mathbf{H} \in \mathbb{R}^{6 \times n \times n}$ [18].

IV. MODELLING OBSTACLES

A point in 3D space can be represented as $\mathbf{p} \in \mathbb{R}^3$. The distance d between a point \mathbf{p}_r on a robot and a point \mathbf{p}_o on an obstacle is

$$d_{ro} = \|\mathbf{p}_o - \mathbf{p}_r\|. \quad (8)$$

The unit vector $\hat{\mathbf{n}}_{ro}$ pointing from \mathbf{p}_r to \mathbf{p}_o is

$$\hat{\mathbf{n}}_{ro} = \frac{\mathbf{p}_o - \mathbf{p}_r}{d_{ro}} = -\hat{\mathbf{n}}_{or} \in \mathbb{R}^3. \quad (9)$$

The time derivative of (9) is

$$\begin{aligned} \dot{d}_{ro} &= \frac{d}{dt} \|\mathbf{p}_o(t) - \mathbf{p}_r(t)\| \\ &= \hat{\mathbf{n}}_{or}^\top (\dot{\mathbf{p}}_o(t) - \dot{\mathbf{p}}_r(t)) \end{aligned} \quad (10)$$

and $\dot{\mathbf{p}}(t) \in \mathbb{R}^3$ is the velocity of a point.

We know from differential kinematics that the end-effector velocity is $\boldsymbol{\nu}(t) = \mathbf{J}(\mathbf{q}) \dot{\mathbf{q}}(t)$. Furthermore, we can calculate the velocity of any point fixed to the robot by taking the

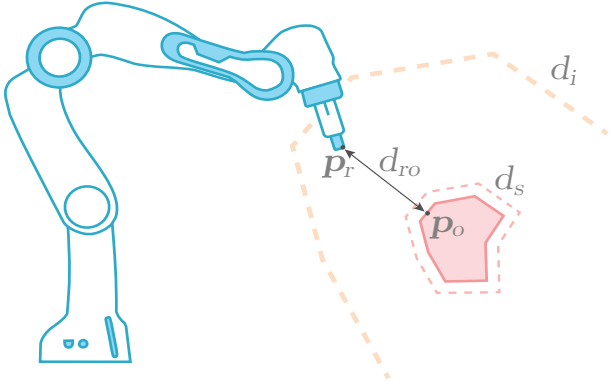


Fig. 2: The distance d_{r_o} from a point on the robot p_r to a point on an obstacle p_o starts to affect the robot motion once d_{r_o} is less than the influence distance d_i . The velocity damper ensures that d_{r_o} is never less than the stopping distance d_s .

translational-velocity component of a modified manipulator Jacobian that considers the point as the robot's end-effector

$$\begin{aligned} \mathbf{J}_p(\mathbf{q}_0 \dots \mathbf{q}_k) &= \Lambda \left(\frac{\partial}{\partial \mathbf{q}_0 \dots \mathbf{q}_k} ({}^0\mathbf{T}_{\mathbf{q}_k} \bullet \mathbf{q}_k \mathbf{T}_P) \right) \\ \mathbf{J}_p(\tilde{\mathbf{q}}) &= \Lambda \left(\frac{\partial}{\partial \tilde{\mathbf{q}}} ({}^0\mathbf{T}_{\mathbf{q}_k} \bullet \mathbf{q}_k \mathbf{T}_P) \right) \end{aligned} \quad (11)$$

where k is the index of the link to which p_r is attached, $\mathbf{J}_p \in \mathbb{R}^{3 \times k}$ is the Jacobian relating the velocity of the point p to the velocities of joints 0 to k , ${}^0\mathbf{T}_{\mathbf{q}_k}$ describes the pose of link k with respect to the base frame of the robot, and \bullet represents composition, and $\Lambda(\cdot)$ is a function that converts the partial derivative of the pose from a tensor $\mathbb{R}^{6 \times k \times k}$ to the translational velocity Jacobian $\in \mathbb{R}^{3 \times k}$. Note that this Jacobian is only a function of the k joints preceding the link to which the point is attached. We denote the set of joints which \mathbf{J}_p is a function of as $\tilde{\mathbf{q}}$ which is of a variable size depending on how many joints there are between the colliding link and the robot base. If the point is attached to the end-effector then $k = n$.

The pose $\mathbf{q}_k \mathbf{T}_P$ describes the fixed point on the robot with respect to the reference frame of link k , and p_r is the origin of frame P . The orientation of this frame is arbitrary, although the direction $\hat{\mathbf{n}}$ is expressed in this frame, so we disregard the angular velocity component from the partial derivative in (11). More details on calculating this Jacobian can be found in [18]. Our provided software package [19] makes it trivial to calculate these Jacobians.

Using (11), we can now write

$$\dot{p}_r(t) = \mathbf{J}_{p_r}(\tilde{\mathbf{q}}) \dot{\tilde{\mathbf{q}}}(t) \quad (12)$$

and the rate of change of distance becomes

$$\begin{aligned} \dot{d}_{r_o}(t) &= \hat{\mathbf{n}}_{or}^\top (\dot{p}_o(t) - \mathbf{J}_{p_r}(\tilde{\mathbf{q}}) \dot{\tilde{\mathbf{q}}}(t)) \\ &= \hat{\mathbf{n}}_{or}^\top \dot{p}_o(t) - \hat{\mathbf{n}}_{or}^\top \mathbf{J}_{p_r}(\tilde{\mathbf{q}}) \dot{\tilde{\mathbf{q}}}(t). \end{aligned} \quad (13)$$

From this we can obtain the distance Jacobian

$$\mathbf{J}_d(\tilde{\mathbf{q}}) = \hat{\mathbf{n}}_{ro}^\top \mathbf{J}_{p_r}(\tilde{\mathbf{q}}) \in \mathbb{R}^6. \quad (14)$$

Substituting (14) into (13) we obtain

$$\mathbf{J}_d(\tilde{\mathbf{q}}) \dot{\tilde{\mathbf{q}}}(t) = \dot{d}_{r_o}(t) - \hat{\mathbf{n}}_{or}^\top \dot{p}_o(t) \quad (15)$$

which is now in a usable form for our QP.

V. OBSTACLE AVOIDANCE

A. Velocity Dampers

The velocity damper approach outlined in [12] prevents robot failure by damping or restricting a velocity before limits are reached. This can be used to restrict joint motion before hitting a limit, or constrain robot velocity before hitting an obstacle. The general velocity damper formula is

$$v \leq \xi \frac{d - d_s}{d_i - d_s} \quad (16)$$

where v is the rate of change of the distance d , ξ is a positive gain which adjusts the aggressiveness of the damper, d_i is the influence distance during which the damper is active, and d_s is the stopping distance in which the distance d will never be able to reach. These distances and are illustrated in Figure 2. When used within an optimizer, v must be found which is less than the limit set by the velocity damper.

We can incorporate obstacle avoidance into the velocity damper as

$$\dot{d}_{r_o}(t) \leq \xi \frac{d - d_s}{d_i - d_s}. \quad (17)$$

However, to use this as an inequality constraint of a QP we must incorporate the form of (15)

$$\mathbf{J}_d(\tilde{\mathbf{q}}) \dot{\tilde{\mathbf{q}}}(t) \leq \xi \frac{d - d_s}{d_i - d_s} - \hat{\mathbf{n}}_{or}^\top \dot{p}_o(t). \quad (18)$$

The effect of (18) is that the optimizer will not choose joint velocities which cause the rate of change of distance between some point on the robot, and some point on an obstacle to decrease. Consequently, the point on the robot and the point on the obstacle will never collide while the damper is active. By adding multiple inequality constraints in the form of (18), the robot can respond to infinitely many dynamic obstacles simultaneously. Multiple obstacles can be incorporated into the same inequality constraint by stacking instances of (18) vertically as

$$\begin{aligned} \mathbf{A} \dot{\tilde{\mathbf{q}}}(t) &\leq \mathbf{b} \quad (19) \\ \begin{pmatrix} \mathbf{J}_{d_0}(\tilde{\mathbf{q}}_0) & \mathbf{0}_{1 \times n - k_0} \\ \vdots & \vdots \\ \mathbf{J}_{d_l}(\tilde{\mathbf{q}}_l) & \mathbf{0}_{1 \times n - k_l} \end{pmatrix} \dot{\tilde{\mathbf{q}}}(t) &\leq \begin{pmatrix} \xi_0 \frac{d_0 - d_s}{d_i - d_s} - \hat{\mathbf{n}}_{or_0}^\top \dot{p}_{o_0}(t) \\ \vdots \\ \xi_l \frac{d_l - d_s}{d_i - d_s} - \hat{\mathbf{n}}_{or_l}^\top \dot{p}_{o_l}(t) \end{pmatrix} \end{aligned}$$

for l obstacles, where the Jacobians within $\mathbf{A} \in \mathbb{R}^{l \times n}$ have been stacked and padded with zeros to make them of constant length n . Obviously, given multiple obstacles and finite degrees-of-freedom, there will exist situations for which there is no viable solution.

If the equality constraint in (6) is active, the robot will be unable to diverge from its path to dodge an obstacle causing the optimizer to fail because it is unable to satisfy both the equality and inequality constraints. To circumvent this, we can add a slack vector to our optimizer.

B. Adding Slack

We can augment our optimization variable $\dot{\mathbf{q}}$ by adding a slack vector $\delta \in \mathbb{R}^6$ and change the problem to

$$\nu(t) - \delta(t) = \mathbf{J}(\mathbf{q})\dot{\mathbf{q}}(t) \quad (20)$$

where δ represents the difference between the desired and actual end-effector velocity – relaxing the trajectory constraint. We reformulate our QP problem to

$$\begin{aligned} \min_{\mathbf{x}} \quad & f_o(\mathbf{x}) = \frac{1}{2}\mathbf{x}^\top \mathbf{Q}\mathbf{x} + \mathbf{C}^\top \mathbf{x}, \\ \text{subject to} \quad & \mathcal{J}\mathbf{x} = \nu, \\ & \mathbf{A}\mathbf{x} \leq \mathbf{B} \\ & \mathcal{X}^- \leq \mathbf{x} \leq \mathcal{X}^+ \end{aligned} \quad (21)$$

where

$$\mathbf{x} = \begin{pmatrix} \dot{\mathbf{q}} \\ \delta \end{pmatrix} \in \mathbb{R}^{(n+6)} \quad (22)$$

$$\mathbf{Q} = \begin{pmatrix} \lambda_q \mathbf{I}_{n \times n} & \mathbf{0}_{6 \times 6} \\ \mathbf{0}_{n \times 6} & \lambda_\delta \mathbf{I}_{6 \times 6} \end{pmatrix} \in \mathbb{R}^{(n+6) \times (n+6)}, \quad (23)$$

$$\mathcal{J} = (\mathbf{J} \quad \mathbf{I}_{6 \times 6}) \in \mathbb{R}^{6 \times (n+6)} \quad (24)$$

$$\mathbf{C} = \begin{pmatrix} \mathbf{J}_m \\ \mathbf{0}_{6 \times 1} \end{pmatrix} \in \mathbb{R}^{(n+6)} \quad (25)$$

$$\mathbf{A} = \begin{pmatrix} \mathbf{J}_{d_0}(\tilde{\mathbf{q}}_0) & \mathbf{0}_{1 \times 6 + n - k_0} \\ \vdots & \vdots \\ \mathbf{J}_{d_l}(\tilde{\mathbf{q}}_l) & \mathbf{0}_{1 \times 6 + n - k_l} \end{pmatrix} \in \mathbb{R}^{(l \times n + 6)} \quad (26)$$

$$\mathbf{B} = \begin{pmatrix} \xi \frac{d_0 - d_s}{d_i - d_s} - \hat{\mathbf{n}}_{or_0}^\top \dot{\mathbf{p}}_{o_0}(t) \\ \vdots \\ \xi \frac{d_l - d_s}{d_i - d_s} - \hat{\mathbf{n}}_{or_l}^\top \dot{\mathbf{p}}_{o_l}(t) \end{pmatrix} \in \mathbb{R}^l \quad (27)$$

$$\mathcal{X}^{-,+} = \begin{pmatrix} \dot{\mathbf{q}}^{-,+} \\ \delta^{-,+} \end{pmatrix} \in \mathbb{R}^{n+6}. \quad (28)$$

We can add to the matrices \mathbf{A} and \mathbf{B} using the velocity damper approach to force the controller to respect joint position limits. We replace \mathbf{A} with

$$\mathbf{A}^* = \begin{pmatrix} \mathbf{A} \\ \mathbf{I}_{n \times n + 6} \end{pmatrix} \in \mathbb{R}^{(l+n) \times (n+6)} \quad (29)$$

and \mathbf{B} with

$$\mathbf{B}^* = \begin{pmatrix} \mathbf{B} \\ \eta \frac{\rho_0 - \rho_s}{\rho_i - \rho_s} \\ \vdots \\ \eta \frac{\rho_n - \rho_s}{\rho_i - \rho_s} \end{pmatrix} \in \mathbb{R}^{l+n} \quad (30)$$

where ρ represents the distance to the nearest joint limit (could be an angle for a revolute joint), ρ_i represents the influence distance in which to operate the damper, and ρ_s represents the minimum distance for a joint to its limit. It should be noted that each row in \mathbf{A}^* and \mathbf{B}^* is only added if the distance, d and ρ , is less than the corresponding influence distance, d_i and ρ_i .

VI. PROPOSED CONTROLLER

Our proposed controller, NEO, exploits the QP described by (21) within a position-based servoing (PBS) scheme. This controller seeks to drive the robot's end-effector in a straight line from its current pose to a desired pose. PBS is formulated as

$$\nu_e = \beta \psi \left(({}^0\mathbf{T}_e)^{-1} \bullet {}^0\mathbf{T}_{e^*} \right) \quad (31)$$

where $\beta \in \mathbb{R}^+$ is a gain term, ${}^0\mathbf{T}_e \in \mathbf{SE}(3)$ is the end-effector pose in the robot's base frame, ${}^0\mathbf{T}_{e^*} \in \mathbf{SE}(3)$ is the desired end-effector pose in the robot's base frame, and $\zeta(\cdot) : \mathbb{R}^{4 \times 4} \mapsto \mathbb{R}^6$ is the function which converts a homogeneous transformation matrix to a spatial twist.

By setting ν in (21) equal to ν_e in (31) the robot will be driven towards the goal, however, not necessarily in a straight line. The robot will diverge from the path to improve manipulability, avoid joint velocity limits, avoid joint position limits, and dodge both static and dynamic obstacles. We detail the effects of changing the controller parameters in Table I.

The proposed controller, while successful in what it proposes, is subject to local minima which can prevent it from reaching the goal pose. We found that encoding a simple *retreat* solution to this proved effective for common cases. If the line of sight between the end-effector and the goal position is broken by the closest obstacle, and the closest obstacle is within the influence distance d_i , then we bias v_x and v_y components of the desired end-effector velocity ν_e to make the arm retreat towards the robot's base frame.

We use our Python library, the Robotics Toolbox for Python [19], to implement our controller. We use the Python library qpsolvers which implements the quadratic programming solver [21] to optimise (21).

VII. EXPERIMENTS

We validate and evaluate our controller by testing on a real manipulator as well as in simulation. In these experiments,

TABLE I: Controller Parameter Description

β	Adjusts how fast the robot's end-effector will travel towards the goal pose. A value too large will cause joint velocity limits to be exceeded while too small increases the time to reach the goal.
λ_q	Adjusts the trade-off between minimising the total joint velocity compared to maximising manipulability. A value too large will cause joint velocity limits to be exceeded while too small reduces the possible manipulability gains.
λ_δ	Adjusts the cost of increasing the total of the slack vector. A gain too large limits the possible additional manipulability achievable, while a gain too small leads to the possibility that the slack will cancel out the desired velocity, leaving a steady-state error.
ξ	Adjusts how aggressively the robot will repel away from obstacles. Too large will cause the joint velocity limits to be exceeded, while too small will reduce obstacle avoidance performance.
η	Adjusts how aggressively the robot will repel away from joint limits. Too large will cause the joint velocity limits to be exceeded, while too small will reduce joint limit avoidance performance.

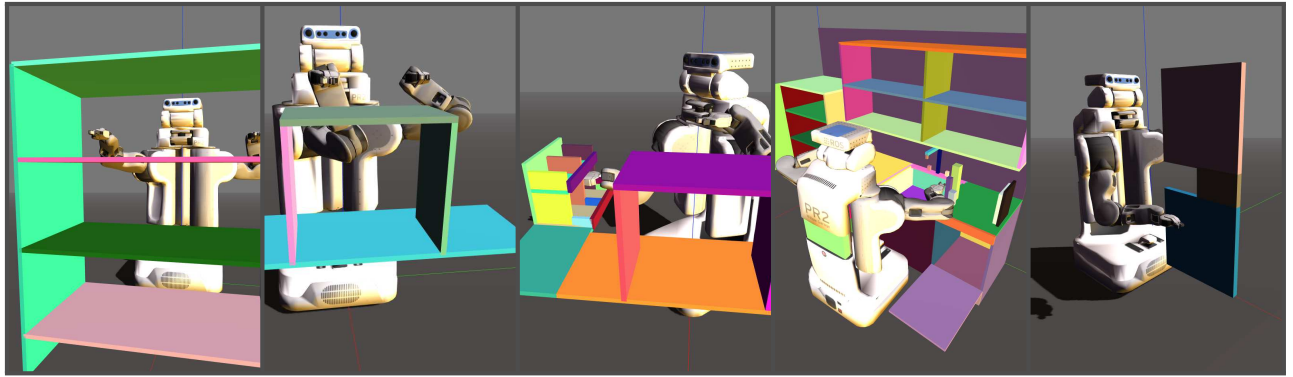


Fig. 3: The five different test scenes in the motion planning benchmark: Bookshelf, Industrial A, Industrial B, Counter, and Tunnel. Images are from Swift [20] and the Robotics Toolbox for Python [19].

NEO has full state information of the environment which otherwise would need to be provided by eye in hand and/or third-person-view cameras with depth sensing capabilities.

We use the following values for the controller parameters: $\xi = 1$, $d_i = 0.3$ m, and $d_s = 0.05$ m in (27), $\eta = 1$, $\rho_i = 50^\circ$, and $\rho_s = 2^\circ$ in (30), $\beta = 1$ in (31), and $\lambda_q = 0.01$, and $\lambda_\delta = \frac{1}{e}$ in (23), where e represents the total error between the current and desired end-effector pose. By setting λ_δ to be inversely proportional to pose error, the optimiser has freedom to maximise manipulability at the beginning of the trajectory while the increasing restriction ensures the end-effector continues to approach the goal. Table I describes each of the gains within NEO, as well as the consequence of making them too large or too small. In practise we found that performance was generally sound within 50% to 200% of the chosen gain values.

For the simulated experiments, we use our open-source simulator Swift [20] to simulate the Willow Garage PR2. For the physical experiments, we use our Python library [19] and ROS middleware to interface with the robot. We use the 7 degree-of-freedom Franka-Emika Panda robot in these experiments.

A. Experiment 1: Physical Robot

We show the merits of NEO by having it operate on a physical Panda manipulator for several different scenarios. In these scenarios, the robot has a desired end-effector pose which it must reach. The tasks reflect grasping scenarios where the end-effector starts high above a table, and the desired end-effector pose is just above the table. However, the robot must dodge one or more non-stationary obstacles present in the environment. This reflects conditions likely if the robot is operating with a human in close proximity or perhaps other robot systems. The scenarios tested are as follows

- a) The robot must servo to a hypothetical grasp target on the table while a sphere of 0.05m radius travels towards the robot with a velocity of 0.2 m/s. If no action is taken, the sphere will collide with the robot's end-effector.
- b) The same as above, except there is a second sphere of 0.05m radius travelling towards the robot's elbow with

a velocity of 0.2 m/s. If no action is taken, the first sphere will collide with the robots end-effector, while the second collides with the elbow.

- c) The same as above, except the desired end-effector pose changes by translating along the table with a velocity of 0.1 m/s for 4 seconds during the task. This represents a scenario where the grasp target has been disturbed. Once again, if no action is taken, the robot will collide with both spheres.

B. Experiment 2: Motion Planning Benchmark

We compare NEO to several state-of-the-art motion planning algorithms on 198 problems over five different test scenes displayed in Figure 3. The test scenes were part of a selection defined by MoveIt! [22], [23]. However, the five selected; Bookshelves, Counter Top, Industrial A, Industrial B, and Tunnel, were the most complex.

In each problem, the robot is initialised in a defined joint configuration. The final position of the robot is defined by another joint configuration. The motion planners must plan between the initial and final configurations. However, NEO does not work by constraining the final joint configuration as it goes against the premise of task-space reactive control to know the final joint configuration. Therefore, NEO is constrained by the end-effector pose of the robot when it is in the specified final joint configuration.

We obtained the definition of the benchmark scenes, initial and target configurations, and motion planning implementations from Trjopt's supplementary material [6]. We compare our results to four motion planners: Trajopt [6], OMPL-RRTConnect [24], and OMPL-LBKPIECE [25], and CHOMP [5].

VIII. RESULTS

The average execution time of the NEO controller during the experiments was 9.8 ms. This was using an Intel i7-8700K CPU with 12 cores at 3.70GHz in a single threaded process. Reducing the execution time is possible through using multithreading techniques as the program is easily parallelizable.

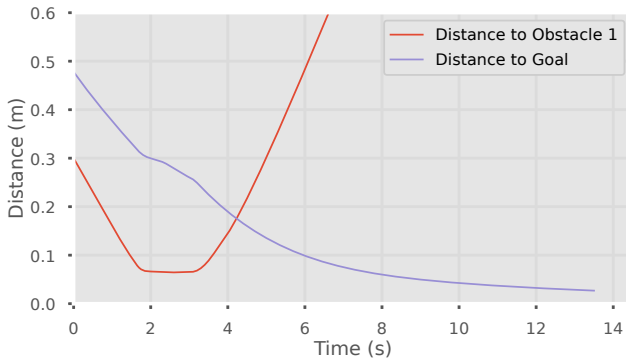


Fig. 4: Experiment 1a: Euclidean distance between robot and obstacle, and robot and goal.

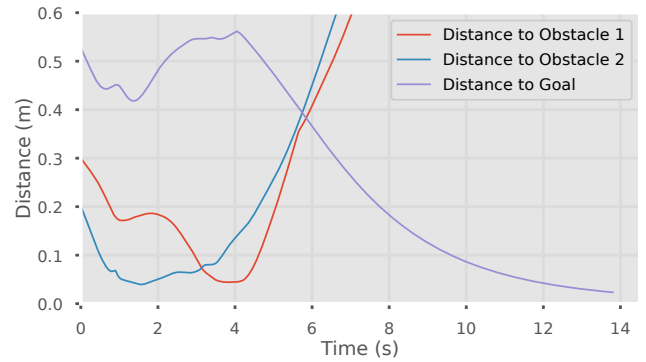


Fig. 6: Experiment 1c: Euclidean distance between robot and obstacles, and robot and goal.

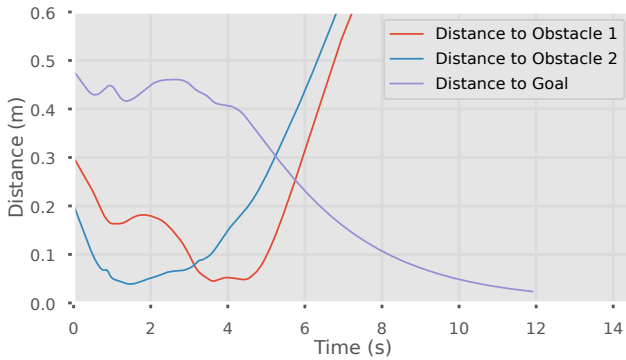


Fig. 5: Experiment 1b: Euclidean distance between robot and obstacles, and robot and goal.

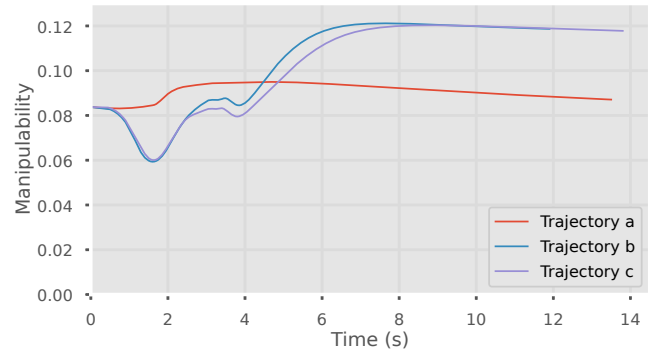


Fig. 7: Experiment 1c: The manipulability of the robot throughout each 3 scenarios.

A. Experiment 1 Results

Scenario a) displayed in Figure 4, shows that once the obstacle gets close to the robot, the robot's end-effector stalls in its progress towards the goal. The distance between the obstacle and the robot never goes below the stopping distance of 5 cm. Once the robot has dodged the obstacle, the robot is free to continue travelling towards the goal pose.

Scenario b) displayed in Figure 5 is more difficult, as there are two obstacles on a collision course with the robot. In this case, obstacle 2 first causes the robot to move from the desired trajectory. As the robot clears it, obstacle 1 enters the robot's path causing another disruption. Both obstacles remain beyond the stopping safety distance.

Scenario c) displayed in Figure 6, shows similar results to scenario b), except that the robot's trajectory has been further interrupted due to the non-stationary goal. Once the goal stops moving, the robot is able to reach it.

Figure 7 displays the manipulability of the robot during each trajectory. This figure clearly shows that despite the complex nature of the robot movement to dodge dynamic obstacles and track a moving goal pose, the manipulability of the robot remains very high.

B. Experiment 2 Results

The results from Experiment 2 are displayed in Table II. These results show that NEO is not capable enough to completely replace fully-featured motion planners in very complex scenarios. However, NEO scored very well in the *Bookshelf* scene successfully completing 44 out of 45 tasks with a 98% success rate. Additionally, in the *Industrial A* scene, NEO completed 50 out of 66 tasks with a 76% success rate. Neo performed less well in the other scenes.

From Figure 3, it is clear that the *Bookshelf* and *Industrial A* scenes contain many large broad obstacles, while *Industrial B* and *Counter* scenes contain many small obstacles with numerous small and enclosed spaces. This suggests that on scenes which do not feature many intricate obstacles with small confined spaces, NEO is a viable alternative for motion planning with the added benefits of reactivity. In more complex environments, especially those containing dynamic obstacles, NEO would ideally be employed as a local controller to deal with dynamic obstacles while a global planner provides the global trajectory.

Another key result from Table II is that NEO takes roughly 10 ms to compute the next action, while the motion planners must compute the whole trajectory before the robot can move. This ranges from 191 ms to 4910 ms for the motion planners. Consequently, they lack the reactivity required

TABLE II: Experiment 2: Motion Planning Benchmark

	NEO (ours)	Trajopt	OMPL- RRTConnect	OMPL-LBKPIECE	CHOMP-HMC
Success	69.7%	81.8%	85.4%	75.8%	65.2%
Average time (ms)	9.8	191	615	1300	4910

to be able to respond to dynamic obstacles, changes in the environment, or even changes to the target pose.

IX. CONCLUSIONS

In this paper we have presented NEO, a novel Expeditious Optimisation Algorithm for manipulator motion control while dodging dynamic and static obstacles, avoiding joint limits, and maximising manipulability. Our experiments show the purely reactive and real-time NEO controller is reliable in environments containing dynamic obstacles reflective of workspaces containing multiple robots working with humans. Additionally, NEO is shown to be viable for general environments containing benches or shelves but will struggle in environments containing small confined spaces with confined spaces and is an area for future work. In such scenarios, NEO is better employed as a local controller when dynamic obstacles are encountered.

Our approach requires the computation of many Jacobians and a Hessian to operate: including the manipulability Jacobian, the manipulator Jacobian (between any points on the robot), the manipulator Hessian, and distance Jacobians. However, the associated Python library, the Robotics Toolbox for Python [19], can calculate and produce all required components. The only required input for our library is a kinematic robot model which can be in standard or modified Denavit–Hartenberg notation, a URDF/XACRO model, or the ETS format [18].

REFERENCES

- [1] T. Yoshikawa, “Manipulability of Robotic Mechanisms,” *The International Journal of Robotics Research*, vol. 4, no. 2, pp. 3–9, 1985.
- [2] S. M. LaValle and J. J. Kuffner Jr, “Randomized kinodynamic planning,” *The international journal of robotics research*, vol. 20, no. 5, pp. 378–400, 2001.
- [3] L. E. Kavraki, P. Svestka, J.-C. Latombe, and M. H. Overmars, “Probabilistic roadmaps for path planning in high-dimensional configuration spaces,” *IEEE transactions on Robotics and Automation*, vol. 12, no. 4, pp. 566–580, 1996.
- [4] M. Kalakrishnan, S. Chitta, E. Theodorou, P. Pastor, and S. Schaal, “Stomp: Stochastic trajectory optimization for motion planning,” in *2011 IEEE International Conference on Robotics and Automation*, 2011, pp. 4569–4574.
- [5] N. Ratliff, M. Zucker, J. A. Bagnell, and S. Srinivasa, “Chomp: Gradient optimization techniques for efficient motion planning,” in *2009 IEEE International Conference on Robotics and Automation*, 2009, pp. 489–494.
- [6] J. Schulman, J. Ho, A. X. Lee, I. Awwal, H. Bradlow, and P. Abbeel, “Finding locally optimal, collision-free trajectories with sequential convex optimization,” in *Robotics: science and systems*, vol. 9, no. 1. Citeseer, 2013, pp. 1–10.
- [8] D. E. Whitney, “Resolved motion rate control of manipulators and human prostheses,” *IEEE Transactions on Man-Machine Systems*, vol. 10, no. 2, pp. 47–53, June 1969.
- [7] S. K. Chan and P. D. Lawrence, “General inverse kinematics with the error damped pseudoinverse,” in *Proceedings. 1988 IEEE International Conference on Robotics and Automation*. IEEE, 1988, pp. 834–839.
- [9] J. Park, W. Chung, and Y. Youm, “Computation of gradient of manipulability for kinematically redundant manipulators including dual manipulators system,” *Transactions on Control, Automation and Systems Engineering*, vol. 1, no. 1, pp. 8–15, 1999.
- [10] D. J. Agravante, G. Claudio, F. Spindler, and F. Chaumette, “Visual servoing in an optimization framework for the whole-body control of humanoid robots,” *IEEE Robotics and Automation Letters*, vol. 2, no. 2, pp. 608–615, 2017.
- [11] J. Haviland and P. Corke, “A purely-reactive manipulability-maximising motion controller,” *arXiv preprint arXiv:2002.11901*, 2020.
- [12] B. Faverjon and P. Tournassoud, “A local based approach for path planning of manipulators with a high number of degrees of freedom,” in *Proceedings. 1987 IEEE International Conference on Robotics and Automation*, vol. 4, 1987, pp. 1152–1159.
- [13] O. Khatib, “Real-time obstacle avoidance for manipulators and mobile robots,” in *Autonomous robot vehicles*. Springer, 1986, pp. 396–404.
- [14] S. Hutchinson, G. D. Hager, and P. I. Corke, “A tutorial on visual servo control,” *IEEE Transactions on Robotics and Automation*, vol. 12, no. 5, pp. 651–670, Oct 1996.
- [15] D. Morrison, J. Leitner, and P. Corke, “Closing the loop for robotic grasping: A real-time, generative grasp synthesis approach,” in *Robotics: Science and Systems XIV*. Robotics: Science and Systems Foundation, June 2018.
- [16] J. Nocedal and S. Wright, *Numerical optimization*. Springer Science & Business Media, 2006.
- [17] P. Corke, *Robotics, Vision and Control*, 2nd ed. Springer International Publishing, 2017.
- [18] J. Haviland and P. Corke, “A systematic approach to computing the manipulator Jacobian and Hessian using the elementary transform sequence,” *arXiv preprint*, 2020.
- [19] —, “Webpage for the Robotics Toolbox Python software package.” [Online]. Available: <https://github.com/petercorke/robotics-toolbox-python>
- [20] —, “Swift: a Python/JavaScript robotics simulator.” [Online]. Available: <https://github.com/jhavl/swift>
- [21] D. Goldfarb and A. Idnani, “A numerically stable dual method for solving strictly convex quadratic programs,” *Mathematical programming*, vol. 27, no. 1, pp. 1–33, 1983.
- [22] S. Chitta, I. Sukan, and S. Cousins, “Moveit![ros topics],” *IEEE Robotics & Automation Magazine*, vol. 19, no. 1, pp. 18–19, 2012.
- [23] B. Cohen, I. A. Şucan, and S. Chitta, “A generic infrastructure for benchmarking motion planners,” in *2012 IEEE/RSJ International Conference on Intelligent Robots and Systems*. IEEE, 2012, pp. 589–595.
- [24] J. J. Kuffner and S. M. LaValle, “Rrt-connect: An efficient approach to single-query path planning,” in *Proceedings 2000 ICRA. Millennium Conference. IEEE International Conference on Robotics and Automation. Symposia Proceedings (Cat. No. 00CH37065)*, vol. 2. IEEE, 2000, pp. 995–1001.
- [25] I. A. Şucan and L. E. Kavraki, “Kinodynamic motion planning by interior-exterior cell exploration,” in *Algorithmic Foundation of Robotics VIII*. Springer, 2009, pp. 449–464.